ISSN 0038-0946, Solar System Research, 2015, Vol. 49, No. 5, pp. 339–345. © Pleiades Publishing, Inc., 2015.
Original Russian Text © D.E. Ionov, V.I. Shematovich, 2015, published in Astronomicheskii Vestnik, 2015, Vol. 49, No. 5, pp. 373–379.

Hydrogen-Dominated Upper Atmosphere of an Exoplanet: Heating by Stellar Radiation from Soft X-Rays to Extreme Ultraviolet

D. E. Ionov and V. I. Shematovich

Institute of Astronomy, Russian Academy of Sciences, Moscow, Russia

e-mail: shematov@inasan.ru

Received January 13, 2015

Abstract—A study is presented of how the upper atmosphere of a planet is heated by extreme radiation from the parent star, depending on the distribution of the radiation flux in the soft X-ray and extreme ultraviolet (EUV) ranges. Calculations are performed to find the efficiency of heating by stellar X-ray to EUV radiation in a hydrogen-dominated upper atmosphere for the extrasolar gas giant HD 209458b. It is shown that heating efficiency by extreme stellar UV radiation in a hydrogen-dominated upper atmosphere does not exceed 20–25% at the main thermospheric heights given that the calculation takes into account the photoelectron impact. It is found that an increase in the X-ray flux by several orders of magnitude leads to a slight decrease in the heating efficiency.

Keywords: extrasolar planetary systems, exoplanets, atmospheres

DOI: 10.1134/S0038094615050056

INTRODUCTION

In recent years, astronomers have discovered and studied a large number of exoplanets: as of today, over 1800 planets in more than 1100 stellar systems have been identified. Modern methods allow researchers not only to detect an exoplanet and determine its orbital characteristics but also to obtain information about its atmosphere. Observations of exoplanet transits and antitransits, as well as direct observations, provide the spectra of exoplanet upper atmospheres, which are used to determine their composition, structure, and dynamics. Moreover, researchers continue to study the giant planets in the Solar System: NASA spacecraft *Cassini* is now exploring Saturnian system, and in 2016 NASA spacecraft *Juno* will start the exploration of Jupiter.

The first step in the study of exoplanet atmospheres was to investigate the hydrogen atmospheres of giant planets (Vidal-Madjar et al., 2003; Yelle, 2004; Ksanfomality, 2004a; 2004b). The first exoplanet with a detected atmosphere was one of the most well-known transiting planets HD 209458b. However, the list of planets with a hydrogen atmosphere is not limited to Jupiter-class planets. It is known that the exosphere of any planet, including the Earth, consists of predominantly light gases: hydrogen and helium. It is also known that all planets have a primary hydrogen–helium atmosphere in the initial stage of planetary evolution. However, small-mass Earth-type planets cannot retain light gases; therefore, they lose their primary atmosphere and then develop a secondary one due to outgassing of their mantle. Attempts to study the process of how planets lose their primary atmosphere were made in (Koskinen et al., 2013; Erkaev et al., 2013, Kislyakova et al., 2013; Shaikhislamov et al., 2014).

One of the key factors determining the state of a planetary atmosphere is the heating by stellar radiation. This factor is especially important for hot Jupiters, i.e., giant planets, in orbits close to the parent star. When the first such planets were discovered, it was found that the atmospheres of some of these planets extend beyond the Roche lobe, which causes a powerful hydrodynamic escape of the atmospheric matter. For some of the planets, the Roche lobe is so full that the hydrodynamic escape may lead to a complete evaporation of the planet's atmosphere (Bisikalo et al., 2013). The escape rate is determined by the intensity of atmospheric heating (Bisikalo et al., 2013).

The heating of the upper hydrogen atmosphere is due to the absorption of X-ray and ultraviolet (XUV) radiation from the parent star in the range 1–100 nm. This wavelength range includes extreme ultraviolet (EUV, 10–100 nm) and soft X-rays (X, 1–10 nm). The XUV radiation is absorbed during the ionization of atomic hydrogen and helium and ionization, dissociation, and dissociative ionization of

molecular hydrogen (Shematovich, 2010; Ionov et al., 2014)

$$H_2 + h\nu, \quad (e_p) \rightarrow \begin{cases} H(1s) + H(1s, 2s, 2p) + (e_p) \\ H_2^+ + e + (e_p) \\ H(1s) + H^+ + e + (e_p) \end{cases} \quad (1)$$

$$H, He + h\nu, (e_p) \rightarrow H^+, He^+ + e + (e_p).$$

In this case, some of the energy of the absorbed photon, which is either equal to or greater than the ionization or dissociation energy, goes into the internal energy of the gas, and the rest is converted into the kinetic energy of the reaction products, mostly into the kinetic energy of electrons. If the energy of a fresh photoelectron is sufficiently large, the photoelectron can enter into secondary ionization and excitation reactions with atmospheric components, losing a part of its initial kinetic energy. Another channel in which photoelectrons lose their initial energy is elastic collisions, as a result of which the deposited energy is converted into heat. Thus, photoelectron energy partly goes into the internal energy and partly into heating the atmosphere.

We shall use the following notation: $W_{h\nu}$ is the energy of the UV radiation absorbed per unit time in unit volume; W_{pe} is the initial kinetic energy of the photoelectrons per unit time in unit volume; and W_T is the energy of electrons, per unit time, which goes into heat in unit volume. Detailed expressions for the rates of absorption of stellar UV radiation and the heating of atmospheric gas $W_{h\nu}$, W_{pe}, and W_T are given in (Shematovich et al., 2014). Then, the total coefficient for the heating efficiency is calculated from the formula:

$$\eta_{h\nu}(z) = \frac{W_T(z)}{W_{h\nu}(z)}. \quad (2)$$

Due to reactions, taking into account suprathermal photoelectrons, the real heating efficiency will be less than unity.

However, in the majority of studies on atmospheric escape (Lammer et al., 2003; Baraffe et al., 2004; Lecavelier et al., 2004; Hubbard et al., 2007a; 2007b; Lecavelier, 2007; Davis and Wheatley, 2009; Sanz-Forcada et al., 2010; 2011; Lissauer et al., 2011; Wu and Lithwick, 2013), the heating efficiency coefficient is assumed to be unity. Recently, while studying the evaporation of the hydrogen atmosphere of the planet KIC 12557548b, Kawahara et al. (2013) used a heating efficiency of 0.5. Murray-Clay et al. (2009) arbitrarily chose a heating efficiency of $\eta_{h\nu} = 0.32$. More detailed studies (e.g., Yelle, 2004) showed that the heating efficiency varies in the range 0.4–0.6 at distances of ~1.03–1.05R_p, is close to ~0.2 at ~1.4R_p, and is ~0.15 at distances >1.4R_p, where R_p is the planet's radius. Guided by these studies, some authors believe that this value is approximately 0.3. This is consistent with the results obtained by Watson et al. (1981), who investigated the escape of the hydrogen atmosphere of the early Earth. These values are close to the estimates obtained by Chassefieère (1996) ($\eta_{h\nu} = 0.15$–0.3) in a study of hydrodynamic hydrogen escape in the upper atmosphere of the early Venus.

Other authors use a set of different heating efficiency values in their studies. Thus, Penz et al. (2008) assume $\eta_{h\nu}$ to be 0.1, 0.6, and 1; Lammer et al. (2009): 0.1, 0.25, 0.6, and 1; and Jackson et al. (2010): 0.1, 0.25, 0.5, and 1 (for the planet CoRoT-7b). A year later, Leitzinger et al. (2011) also conducted a study of the same planet CoRoT-7b and the planet Kepler-10b, in which they assumed that $\eta_{h\nu} = 0.25$. Ehrenreich and Dèsert (2011) studied the escape of matter for close-in planets for a heating efficiency of 0.01, 0.15, and 1. Jackson et al. (2012) studied atmospheric heating by X-ray to UV (XUV) radiation under the assumption that the heating efficiency varies in the range 0.25–1. Koskinen et al. (2013) assume that the heating efficiency is 0.1, 0.3, 0.5, 0.8, and 1. In their model, the atmospheric temperature varies in the range 6000–8000 K. It should be noted that the model proposed by Koskinen et al. (2013) does not take into account molecular hydrogen ionization. However, dissociative ionization makes a substantial contribution to atmospheric heating. Moreover, the lower limit of the computational domain in this model does not coincide with the lower boundary of the thermosphere.

Over the last couple of years, there have been several studies on atmospheric escape for the super-Earths and super-Neptunes in the Kepler-11 system (Lopez et al., 2012; 2013), which use a heating efficiency of 0.1–0.2. Kurokawa and Kaltenegger (2013) studied the atmospheric escape of CoRoT-7b and Kepler-10b, using a heating efficiency coefficient similar to the one in (Leitzinger et al., 2011): $\eta_{h\nu} = 0.25$. Valencia et al. (2013) studied the atmospheric escape of the planet GJ 1214b and other sub-Neptunes. The minimum heating efficiency in their study was 0.1 and the maximum was 0.4. The roughly similar extreme values of 0.15 and 0.4 were used in (Erkaev et al., 2013; Lammer et al., 2013; Kislyakova et al., 2013), which study the hydrogen escape for the early Mars, super- and sub-Earths in the habitability zone of solar-type G-stars with XUV-fluxes exceeding the solar flux by a factor of two orders of magnitude, and five exoplanets in the Kepler-11 system, which occupy an intermediate position between super-Earths and sub-Neptunes.

It is evident from this brief overview that different assumptions about heating efficiency give different values ranging from 0 to 1. However, an incorrect estimate for this parameter can change the mass loss rate by an order of magnitude. Therefore, it is so important to calculate the efficiency of heating by XUV radiation for hydrogen atmospheres.

Previously, we calculated the heating efficiency for the atmosphere of the planet HD 209458b (Shematovich et al., 2014) by radiation with a solar spectrum. However, the calculated results are valid only for the planet atmosphere in its modern state, when it is irra-

diated by a star with an age of 4 Gyr. The stellar radiation flux in the X-ray and UV-ranges varies greatly in the course of the stellar evolution. Scientists usually explain this process by the deceleration of the star rotation, which reduces its activity (Linsky and Güdel, 2015). Thus, the heating of the planet's atmosphere should change during the evolution of the parent star. Figure 1.8 in (Linsky and Güdel, 2015) shows how the UV and X-ray radiation flux changes for stars of various ages. For young stars, the flux at 0.1–120 nm is much greater than the solar flux. Nevertheless, the intensity may differ by several orders of magnitude between bands. Thus, for stars with an age of 0.1 Gyr, the flux at wavelengths of 0.1 nm is greater than the solar flux by a factor of about 2000, while that at 100 nm for stars of the same age is greater than the solar flux by a factor of only 30. At the same time, the flux is strongly nonlinearin dependence on frequency. For all the frequencies in the EUV range, the flux increases at about the same rate with decreasing star age while the flux at 1–2 nm exceeds these values by several orders of magnitude. In particular, the flux ratio for the stars EK Dra (0.1 Gyr) and β Hyi (6.7 Gyr) is 20000 at a wavelength of 1 nm, 200 at a wavelength of 10 nm, and only 50 at a wavelength of 100 nm.

Thus, to solve the problem of stability of hot Jupiter atmospheres at cosmological timescales, we need to understand how atmospheric heating changes depending on the stellar spectrum. In this study, we examined the change in the intensity and heating efficiency profiles with the changing power distribution in the XUV spectrum of the parent star.

MODEL

The transfer and kinetics of photoelectrons in the hydrogen- and helium-dominated upper atmosphere of an (exo)planet was calculated using a Monte Carlo model (Shematovich et al., 2008; Shematovich, 2010) adapted to hydrogen atmospheres. In the daytime upper atmosphere, high-energy electrons are formed by photoionization of the main atmospheric components by EUV and soft X-ray stellar radiation. The resulting electrons are transferred in the upper atmosphere, where they lose their kinetic energy in elastic, nonelastic, and ionization collisions with the main components of the surrounding atmospheric gas

$$e(E) + X \rightarrow \begin{cases} e(E') + X \\ e(E') + X^* \\ e(E') + X^+ + e(E_s), \end{cases} \quad (3)$$

where E and E' are the kinetic energies of the primary electron before and after the collision; X^* and X^+ are atmospheric components in the excited and ionized states. Here, E_s is the energy of the secondary electron formed in the subsequent ionization collision. The energy E_s is selected according to the procedure described in (Garvey and Green, 1976; Jackman et al., 1977; Garvey et al., 1977). Photoelectrons with suprathermal energies lose their excess kinetic energy in collisions (3) with the surrounding atmospheric gas. Accordingly, the kinetics and transport of photoelectrons is described by the Boltzmann equation:

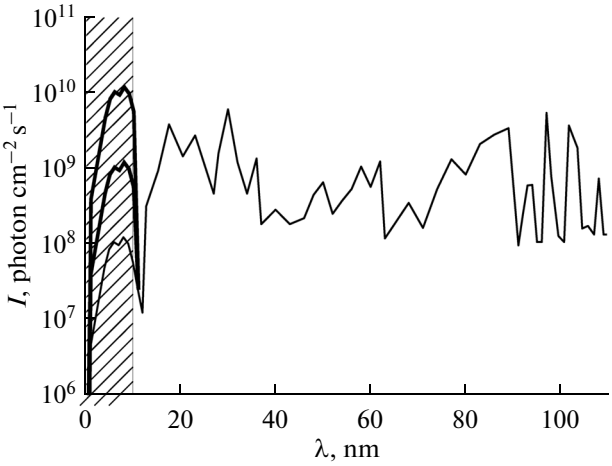

Fig. 1. Radiation flux at different wavelengths for all the three variants of the spectrum. The dashed area shows the soft X-ray range with a wavelength of 1–10 nm. Solid lines show the spectra with a flux in soft X-rays, which is increased by a factor of 10 and 100.

$$\vec{v}\frac{\partial}{\partial \vec{r}} f_e + \frac{\vec{Y}}{m_e}\frac{\partial}{\partial \vec{v}} f_e = Q_{e,\text{photo}}(\vec{v}) + Q_{e,\text{secondary}}(\vec{v}) + \sum_{M=\text{H,He,H}_2} J(f_e, f_M), \quad (4)$$

where r, v, and Y are the radius, velocity, and force-field vectors, and $f_e(\vec{r},\vec{v})$ and $f_M(\vec{r},\vec{v})$ are the velocity distribution functions for electrons and components of the surrounding atmospheric gas, respectively. The transport of electrons in the planetary force field $\vec{Y}$ is described in the left-hand part of the equation. The term $Q_{e,\text{photo}}$ in the right-hand part of the kinetic equation describes the formation rate of fresh electrons due to photoionization, and the term $Q_{e,\text{secondary}}$ describes the formation of secondary electrons due to the ionization by photoelectrons The collision integrals for elastic and nonelastic interactions of electrons with the surrounding atmospheric gas $J(f_e,f_M)$ are written in the standard form under the assumption that atmospheric gas is characterized by a local-equilibrium Maxwellian velocity distribution.

A detailed description of the Monte Carlo model of photoelectron transport in a planetary atmosphere is given in (Marov et al., 1996; Shematovich et al., 2008; Shematovich, 2010). Here, we only emphasize that this model uses the experimental and calculated data for cross-sections and distributions of scattering angles in elastic, inelastic, and ionization collisions of electrons with H_2, He, and H, which were selected from the sources listed in (Shematovich, 2010). The partial

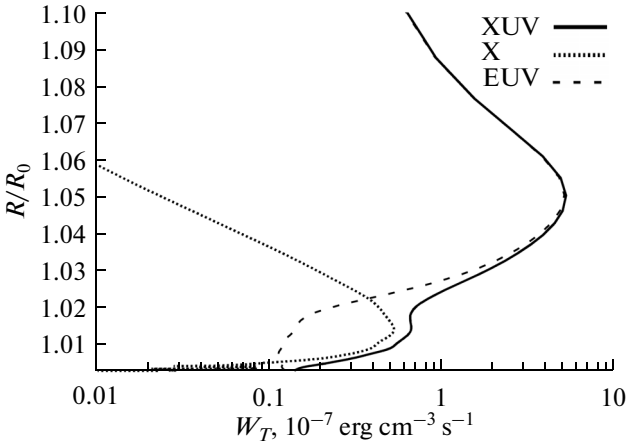

Fig. 2. Profiles of the for atmospheric heating intensity by stellar radiation for a solar spectrum and separately for X-ray and EUV ranges. The dotted line shows the heating intensity by X-ray radiation. The dashed line shows the heating intensity by EUV radiation. The solid line shows the heating by radiation with the total solar XUV spectrum.

and total rates of ionization by a photoelectron flux are given by the standard formulas on the basis of the calculated distribution functions $f_e(r, v)$ of the thermosphere electrons.

The object of research was the planet HD 209458b, the first discovered hot Jupiter, for which there are results of several observations and abundant atmospheric simulation data. The stellar spectrum in the UV range is considered to be similar to that of the modern Sun. The spectrum used in the study is shown in Fig. 1. The shaded area shows the soft X-ray range, in which the intensity changes with the age of the star.

The model calculates the rate of radiation and photoelectron energy transfer into internal energy in each of photoreaction energy transfer (1) and secondary-electron reactions (3). A separate calculation is made for the energy of suprathermal photoelectrons that goes into heating energy. Thus, the simulation results can be used to determine the total heating efficiency and the efficiency of heating by photoelectrons and figure out what processes have the greatest effect on atmospheric heating.

We carried out several calculations using different stellar radiation spectra. In all the models, we used the results published in (Yelle, 2004) as initial distribution profiles for neutral components and temperature.

According to (Linsky and Güdel, 2015), the radiation intensity changes differently with time in the soft X-ray and EUV ranges. In both bands the flux is greater for young stars than for the solar-age ones; however, in X rays this difference is about three orders of magnitude, while in the EUV range it is only an order of magnitude. Thus, in the early epochs, the intensity ratio in the X-ray and EUV ranges was an order of magnitude greater that the corresponding value for the modern Sun.

The spectrum of the radiation affecting the planet's atmosphere was changing as follows. The flux increase as such would lead to a fold change in heating intensity, but the pattern of the intensity profile should not change. Therefore, the radiation flux in the EUV range 10–100 nm was virtually the same for all the models, but the flux in the range 1–10 nm increased by a factor of 10 and 100, respectively.

Thus, we carried out calculations for the following five models.

(1) Basic model (1XUV), which uses the solar spectrum (Huebner et al., 1992) calculated for the orbital distance of the exoplanet being studied (r = 0.045 AU for HD 209458b).

(2) EUV. To determine the role of EUV radiation in atmospheric heating, we conducted a simulation with a solar-type spectrum only in the range 10–100 nm. The radiation intensity at 1–10 nm was assumed to be zero.

(3) X (soft X-rays). To determine the role of the more short-wave part of XUV radiation in atmospheric heating, we conducted a simulation with a solar-type spectrum only in the range 1–10 nm, i.e., in soft X-rays only. The radiation intensity at 10–100 nm was assumed to be zero.

(4) 10X. In the range 10–100 nm, the spectrum is similar to the solar one at the corresponding orbital distance. In the range 1–10 nm, i.e., soft X-rays, the radiation intensity is multiplied by a factor of 10.

(5) 100X. The spectrum is built on the same principle as in the 10X model, but the multiplication factor is 100.

RESULTS OF CALCULATIONS

Figure 2 shows the profile of atmospheric heating intensity in the basic model (solid line) and for the EUV (dashed line) and X (dotted line) models. It is evident that UV- and X rays are absorbed at different heights, which is why the heating intensity profile in the basic model has two peaks. UV-rays are absorbed at a height of 1.06 R_p. Soft X rays are absorbed at a height of 1.02 R_p. In the basic model, the lower-height peak has a lower intensity due to the relatively low stellar luminosity in X rays. This situation changes in different models.

Figure 3 shows the absorption intensities $W_{h\nu}$ (upper panel) for the stellar XUV radiation and atmospheric gas heating W_T (lower panel) for the models 1X (solid line), 10X (dashed line), and 100X (dotted line). It is evident that an increase in radiation intensity in X rays leads to an increase in the corresponding peak in the intensity profile, which is at a height of $1.02R_p$. Both of the peaks for the 10X model have almost the same height; the 100X profile has only one maximum at lower heights, whose magnitude has grown. Thus, a change in the stellar spectrum leads to a dramatic change in the heating intensity profile: for low inten-

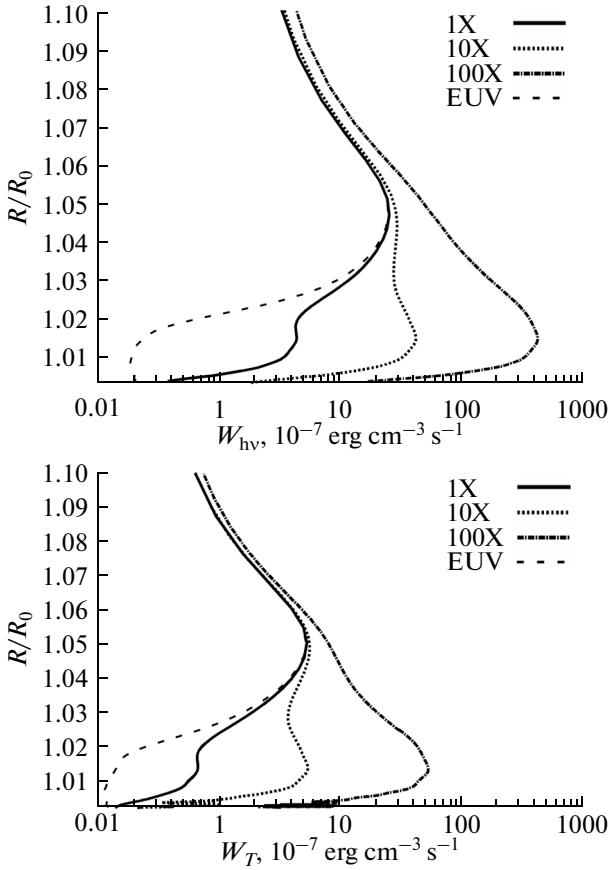

Fig. 3. Absorption intensity $W_{h\nu}$ (upper panel) of the stellar XUV radiation and atmospheric gas heating W_T (lower panel) for the XUV (solid line), 10X (dashed line), and 100X (dotted line) models.

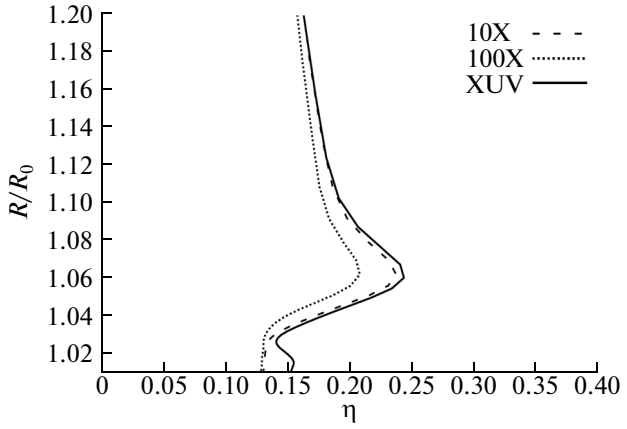

Fig. 4. Total heating efficiency for a hydrogen-dominated upper atmosphere in the 1X (solid lines), 10X (dashed lines), and 100X (dotted lines) models.

sity in the short-wave spectrum, heating occurs at a height of $1.06R_p$; when the intensity is greater by a factor of 100, the radiation heats the atmosphere almost near the planet's photometric radius. Although, the height of the heating peak shifts inward by only $0.02R_p$, this may lead to a substantial change in the energy balance of the atmosphere due to the exponential nature of the height dependence of gas density.

In these circumstances, it is interesting to consider the behavior of the heating efficiency. Figure 4 shows the total heating efficiency $\eta_{h\nu}$ profiles for the models 1X (solid line), 10X (dashed line), and 100X (dotted line). It is evident that despite the changes in the spectrum and heating intensity, there are no substantial changes in the heating efficiency profile. Moreover, the lowest values of the heating efficiency coefficient are observed at a height of about $1.02R_p$, which is characterized by the largest changes in heating intensity. The heating efficiency profile has a peak at a height of $1.06R_p$.

It is evident from Fig. 4 that an increase in radiation flux in X rays leads to a slight decrease in heating efficiency. This phenomenon can be understood by considering the partial heating efficiencies calculated separately for the soft X ray and EUV ranges (Fig. 5).

The dashed line in this figure shows the partial heating efficiency calculated for the EUV spectrum model i.e., $\left(\frac{W_T^{(\mathrm{EUV})}(z)}{W_{h\nu}(z)}\right)$, and the dotted line shows the partial efficiency for the X model (soft X rays; $\frac{W_T^{(\mathrm{X})}(z)}{W_{h\nu}(z)}$). In this case, $W_T^{(\mathrm{EUV})}(z) + W_T^{(\mathrm{X})}(z) = W_T(z)$. The heating efficiency of atmospheric gas in soft X rays is lower than in the EUV range or the basic XUV spectrum. Therefore, with the increase in the fraction of X rays in the parent star's spectrum, the heating efficiency profile becomes more similar to the X model profile; i.e., the total heating efficiency decreases.

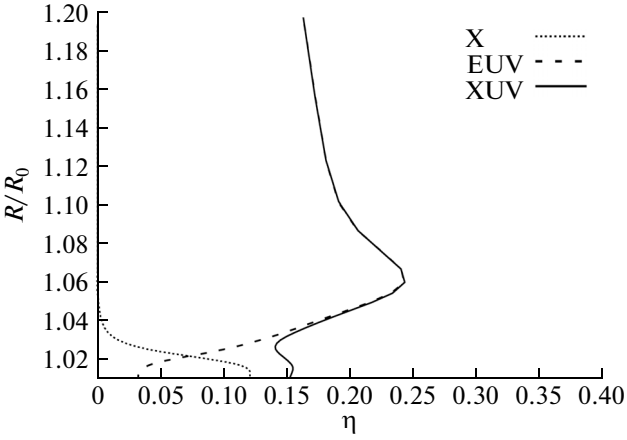

Fig. 5. Total heating efficiency for the basic XUV model (solid line) and its components: the EUV (dashed line) and X (soft X rays, dotted line) models.

CONCLUSIONS

The calculated results for the heating efficiency in the atmosphere of the planet HD 209458b (Shematovich et al., 2014), which is heated by radiation with a solar spectrum, are valid only for the atmosphere of this planet in its modern state, when it is exposed to radiation from the parent star with an age of 4 Gyr. Stellar radiation fluxes in X-ray and UV ranges change substantially during the stellar evolution (Linsky and Güdel, 2015). Therefore, the heating of the planet's atmosphere should also change during the stellar evolution, which may affect the stability of hot Jupiters' atmospheres at cosmological timescales.

In this work, we examine the heating intensity and efficiency profiles for a relative redistribution of energy between soft X-ray and EUV ranges in the XUV spectrum of the parent star, depending on the star's age. We found that the heating efficiency profiles obtained for the solar spectrum with an increase in the radiation flux by a factor of 10 and 100 in the soft X-ray range 1–10 nm do not differ substantially (Fig. 4) from the efficiency profile for the standard solar spectrum (Shematovich et al., 2014). Therefore, the calculated heating efficiencies can be applied to stars younger than the Sun after scaling the photon flux in the soft X-ray and EUV ranges according to the observational data on stellar spectra (Linsky and Güdel, 2015). The results will make it possible to estimate the rate of atmospheric escape for planets in orbit around young stars whose spectrum differs from that of the Sun. To obtain a more comprehensive picture of how changes in the stellar spectrum affect the atmospheric structure and dynamics, we plan to conduct a simulation taking into account the gas dynamics of the atmosphere and the chemical reactions in the gas.

ACKNOWLEDGMENTS

This work was supported by the Russian Foundation for Basic Research, project nos. 14-02-31605 and 14-02-00838.

REFERENCES

Baraffe, I., Selsis, F., Chabrier, G., Barman, T.S., Allard, F., Hauschildt, P.H., and Lammer, H., The effect of evaporation on the evolution of close-in giant planets, *Astron. Astrophys.*, 2004, vol. 419, pp. L13–L16.

Bisikalo, D., Kaygorodov, P., Ionov, D., Shematovich, V., Lammer, H., and Fossati, L., 3D gas dynamic simulation of the interaction between the exoplanet WASP-12b and its host star, *Astrophys. J.*, 2013a, vol. 764, p. 19.

Bisikalo, D.V., Kaigorodov, P.V., Ionov, D.E., and Shematovich, V.I., Types of gaseous envelopes of "hot Jupiter" exoplanets, *Astron. Rep.*, 2013b, vol. 90, p. 715.

Chassefière, E., Hydrodynamic escape of hydrogen from a hot water-rich atmosphere: the case of Venus, *J. Geophys. Res.*, 1996, vol. 101, pp. 26039–26056.

Davis, T.A. and Wheatley, P.J., Evidence for a lost population of close-in exoplanets, *Mon. Notic. Roy. Astron. Soc.*, 2009, vol. 396, pp. 1012–1017.

Ehrenreich, D. and Dèsert, J.-M., Mass-loss rates for transiting exoplanets, *Astron. Astrophys.*, 2011, vol. 529, p. A136.

Erkaev, N.V., Lammer, H., Odert, P., Kulikov, Yu.N., Kislyakova, K.G., Khodachenko, M.L., Güdel, M., Hanslmeier, A., and Biernat, H., XUV-exposed, nonhydrostatic hydrogen-rich upper atmospheres of terrestrial planets. Pt. I: Atmospheric expansion and thermal escape, *Astrobiology*, 2013, vol. 13, pp. 1011–1029.

Garvey, R.H. and Green, A.E.S., Energy-apportionment techniques based upon detailed atomic cross sections, *Phys. Rev. A*, 1976, vol. 14, pp. 946–953.

Garvey, R.H., Porter, H.S., and Green, A.E.S., An analytic degradation spectrum for H2, *J. Appl. Phys.*, 1977, vol. 48, pp. 190–193.

Hubbard, W.B., Hattori, M.F., Burrows, A., and Hubeny, I., A mass function constraint on extrasolar giant planet evaporation rates, *Astrophys. J.*, 2007a, vol. 658, pp. L59–L62.

Hubbard, W.B., Hattori, M.F., Burrows, A., Hubeny, I., and Sudarsky, D., Effects of mass loss for highly-irradiated giant planets, *Icarus*, 2007b, vol. 187, pp. 358–364.

Huebner, W.F., Keady, J.J., and Lyon, S.P., Solar photorates for planetary atmospheres and atmospheric pollutants, *Astrophys. Space Sci.*, 1992, vol. 195, pp. 1–294.

Ionov, D.E., Bisikalo, D.V., Shematovich, V.I., and Hubert, B., Ionization fraction in the thermosphere of the exoplanet HD 209458b, *Solar Syst. Res.*, 2014, vol. 48, no. 2, pp. 105–112.

Jackman, C.H., Garvey, R.H., and Green, A.E.S., Electron impact on atmospheric gases. I – updated cross sections, *J. Geophys. Res.*, 1977, vol. 82, pp. 5081–5090.

Jackson, B., Miller, N., Barnes, R., Raymond, S.N., Fortney, J.J., and Greenberg, R., The roles of tidal evolution and evaporative mass loss in the origin of CoRoT-7 b, *Mon. Notic. Roy. Astron. Soc.*, 2010, vol. 407, pp. 910–922.

Jackson, A.P., Davis, T.A., and Wheatley, P.J., The coronal X-ray-age relation and its implications for the evaporation of exoplanets, *Mon. Notic. Roy. Astron. Soc.*, 2012, vol. 422, pp. 2024–2043.

Kawahara, H., Hirano, T., Kurosaki, K., Ito, Y., and Ikoma, M., Starspots-transit depth relation of the evaporating planet candidate KIC 12557548b, *Astrophys. J.*, 2013, vol. 776, p. L6.

Kislyakova, K.G., Lammer, H., Holmstrom, M., Panchenko, M., Odert, P., Erkaev, N.V., Leitzinger, M., Khodachenko, M.L., Kulikov, Yu.N., Güdel, M., and Hanslmeier, A., XUV-exposed, non-hydrostatic hydrogen-rich upper atmospheres of terrestrial planets. Pt. II: Hydrogen coronae and ion escape, *Astrobiology*, 2013, vol. 13, pp. 1030–1048.

Koskinen, T.T., Harris, M.J., Yelle, R., and Lavvas, P., The escape of heavy atoms from the ionosphere of HD209458b. I. A photochemical-dynamical model of the thermosphere, *Icarus*, 2013, vol. 226, pp. 1678–1694.

Ksanfomaliti, L.V., On the nature of the object HD 209458b: conclusions drawn from comparison of

experimental and theoretical data, *Solar Syst. Res.*, 2004a, vol. 38, no. 4, pp. 300–308.

Ksanfomality, L.V., Regularity of extrasolar planetary systems and the role of the star metallicity in the formation of planets (review), *Solar Syst. Res.*, 2004b, vol. 38, no. 5, pp. 372–382.

Kurokawa, H. and Kaltenegger, L., Atmospheric mass-loss and evolution of short-period exoplanets: the examples of CoRoT-7b and Kepler-10b, *Mon. Notic. Roy. Astron. Soc.*, 2013, vol. 433, pp. 3239–3245.

Lammer, H., Selsis, F., Ribas, I., Guinan, E.F., Bauer, S.J., and Weiss, W.W., Atmospheric loss of exoplanets resulting from stellar X-ray and extreme-ultraviolet heating, *Astrophys. J.*, 2003, vol. 598, pp. L121–L126.

Lammer, H., Odert, P., Leitzinger, M., Khodachenko, M.L., Panchenko, M., Kulikov, Yu.N., Zhang, T.L., Lichtenegger, H.I.M., Erkaev, N.V., Wuchterl, G., Micela, G., Penz, T., Biernat, H.K., Weingrill, J., Steller, M., Ottacher, H., Hasiba, J., and Hanslmeier, A., Determining the mass loss limit for close-in exoplanets: what can we learn from transit observations?, *Astron. Astrophys.*, 2009, vol. 506, pp. 399–410.

Lammer, H., Erkaev, N.V., Odert, P., Kislyakova, K.G., Leitzinger, M., and Khodachenko, M.L., Probing the blow-off criteria of hydrogen-rich 'super-Earths', *Mon. Notic. Roy. Astron. Soc.*, 2013, vol. 430, pp. 1247–1256.

Lecavelier des Etangs, A., Vidal-Madjar, A., McConnell, J.C., and Hébrard, G., Atmospheric escape from hot Jupiters, *Astron. Astrophys.*, 2004, vol. 418, pp. L1–L4.

Lecavelier des Etangs, A., A diagram to determine the evaporation status of extrasolar planets, *Astron. Astrophys.*, 2007, vol. 461, pp. 1185–1193.

Leitzinger, M., Odert, P., Kulikov, Yu.N., Lammer, H., Wuchterl, G., Penz, T., Guarcello, M.G., Micela, G., Khodachenko, M.L., Weingrill, J., Hanslmeier, A., Biernat, H.K., and Schneider, J., Could CoRoT-7b and Kepler-10b be remnants of evaporated gas or ice giants?, *Planet. Space Sci.*, 2011, vol. 59, pp. 1472–1481.

Linsky, J.L. and Güdel, M., Exoplanet host star radiation and plasma environment, in *Characterizing Stellar and Exoplanetary eEnvironments*, Lammer, H. and Khodachenko, M., Eds., Springer, Astrophys. and Space Sci. Lib., 2015, vol. 411, pp.105–136.

Lissauer, J.J., Fabrycky, D.C., Ford, E.B., and 36 coauthors, A closely packed system of low-mass, low-density planets transiting Kepler-11, *Nature*, 2011, vol. 470, pp. 53–58.

Lopez, E.D., Fortney, J.J., and Miller, N., How thermal evolution and mass-loss sculpt populations of super-Earths and sub-Neptunes: application to the Kepler-11 system and beyond, *Astrophys. J.*, 2012, vol. 761, p. id. 59.

Lopez, E.D. and Fortney, J.J., The role of core mass in controlling evaporation: the Kepler radius distribution and the Kepler-36 density dichotomy, *Astrophys. J.*, 2013, vol. 776, p. id. 2.

Marov, M.Ya., Shematovich, V.I., and Bisikalo, D.V., Nonequilibrium processes in the planetary and cometary atmospheres. A kinetic approach to modeling, *Space Sci. Rev.*, 1996, vol. 76, pp. 1–200.

Murray-Clay, R.A., Chiang, E.I., and Murray, N., Atmospheric escape from hot Jupiters, *Astrophys. J.*, 2009, vol. 693, pp. 23–42.

Penz, T., Erkaev, N.V., Kulikov, Yu.N., Langmayr, D., Lammer, H., Micela, G., Cecchi-Pestellini, C., Biernat, H.K., Selsis, F., Barge, P., Deleuil, M., and Léger, A., Mass loss from "hot Jupiters"—implications for CoRoT discoveries. Pt. II: Long time thermal atmospheric evaporation modeling, *Planet. Space Sci.,* 2008, vol. 56, pp. 1260–1272.

Sanz-Forcada, J., Ribas, I., Micela, G., Pollock, A.M.T., García-Álvarez, D., Solano, E., and Eiroa, C., A scenario of planet erosion by coronal radiation, *Astron. Astrophys.*, 2010, vol. 511, p. id. L8.

Sanz-Forcada, J., Micela, G., Ribas, I., Pollock, A.M.T., Eiroa, C., Velasco, A., Solano, E., and García-Álvarez, D., Estimation of the xuv radiation onto close planets and their evaporation, *Astron. Astrophys.*, 2011, vol. 532, p. id. A6.

Shaikhislamov, I.F., Khodachenko, M.L., Sasunov, Yu.L., Lammer, H., Kislyakova, K.G., and Erkaev, N.V., Atmosphere expansion and mass loss of close-orbit giant exoplanets heated by stellar XUV. I. Modeling of hydrodynamic escape of upper atmospheric material, *Astrophys. J.*, 2014, vol. 795, p. id. 132.

Shematovich, V.I., Bisikalo, D.V., Gérard, J.-C., Cox, C., Bougher, S.W., and Leblanc, F., Monte Carlo model of electron transport for the calculation of Mars dayglow emissions, *J. Geophys. Res.*, 2008, vol. 113, p. E02011.

Shematovich, V.I., Supratermal hydrogen produced by the disassociation of molecular hedrogen in the extended atmosphere of exoplanet HD209458b, *Solar Syst. Res.*, 2010, vol. 44, no. 2, pp. 96–103.

Shematovich, V.I., Ionov, D.E., and Lammer, H., Heating efficiency in hydrogen-dominated upper atmospheres, *Astron. Astrophys.*, 2014, vol. 571, p. id. A94.

Valencia, D., Guillot, T., Parmentier, V., and Freedman, R.S., Bulk composition of GJ 1214b and other sub-neptune exoplanets, *Astrophys. J.*, 2013, vol. 775, p. id. 10.

Vidal-Madjar, A., Lecavelier des Etangs, A., Desert, J.-M., Ballester, G.E., Ferlet, R., Hébrard, G., and Mayor, M., An extended upper atmosphere around the extrasolar planet HD209458b, *Nature*, 2003, vol. 422, pp. 143–146.

Watson, A.J., Donahue, T.M., and Walker, J.C.G., The dynamics of a rapidly escaping atmosphere – applications to the evolution of Earth and Venus, *Icarus*, 1981, vol. 48, pp. 15–31.

Wu, Y. and Lithwick, Y., Density and eccentricity of Kepler planets, *Astrophys. J.*, 2013, vol. 772, p. id. 74.

Yelle, R., Aeronomy of extra-solar giant planets at small orbital distances, *Icarus*, 2004, vol. 170, pp. 167–179.

Translated by A. Kobkova